Advanced Modulation Format Generation using High-Speed Directly Modulated Lasers for Optical Metro/Access Systems

Chun-Kit Chan, Wei Jia, and Zhixin Liu
Dept. of Information Engineering, the Chinese University of Hong Kong, Shatin, N.T. Hong Kong SAR, China
Tel: +852-2609-8354, Fax: +852-2603-5032, Email: *ckchan@ie.cuhk.edu.hk*

ABSTRACT

We propose and experimentally demonstrate the generation of various modulation formats using a directly modulated chirp-managed laser (CML), including phase-shaped binary transmission (PSBT), inverse-return-to-zero duobinary (IRZ-duobinary), Manchester-duobinary, return-to-zero differential phase shift keying (RZ-DPSK) and return-to-zero differential quadrature phase-shift-keying (RZ-DQPSK). The CML-based modulation formats improved dispersion tolerance and their corresponding transmitters have the features of compactness, low power consumption and cost-effectiveness, which are desired in metro/access networks. System applications of such formats are also studied.

Keywords: direct modulation, chirp managed laser, modulation format, metro/access network.

1. INTRODUCTION

Optical metro/access networks with network span less than 200 km are best enabled by dispersion tolerant signal modulation formats and cost-effective optical transceivers. Chirp managed laser (CML) [1], which integrates a directly modulated distributed feedback (DFB) laser and an optical band pass filter, is a promising candidate to realize a high-speed optical transmitter for such metro/access applications. It has the advantages of compactness, low cost, high performance and reduced power consumption. Besides, the inherent simultaneous intensity and phase coding property of the directly modulated CML have been exploited to generate various advanced modulation format at 10-Gb/s and above [2].

In this paper, we discuss the generation of various advanced modulation formats including phase-shaped binary transmission (PSBT), inverse-return-to-zero (IRZ) duobinary, Manchester duobinary, return-to-zero differential phase shift keying (RZ-DPSK) and return-to-zero differential quadrature phase-shift-keying (RZ-DQPSK) signals by directly modulating a CML with our designed electrical driving signals. Compared with the conventional signal generation schemes using external modulators, the proposed schemes not only simplify the electronic encoders, but also minimize

Optical Transmission Systems, Subsystems, and Technologies IX, edited by Xiang Liu, Ernesto Ciaramella, Naoya Wada, Nan Chi, Proc. of SPIE-OSA-IEEE Asia Communications and Photonics, SPIE Vol. 8309, 83090X · © 2011 SPIE-OSA-IEEE · CCC code: 0277-786X/11/$18 · doi: 10.1117/12.900452

or even eliminate the costly and bulky external modulators. The performance of the CML-based signal format generation and their applications in optical metro/access networks are also discussed.

2. OPERATION PRINCIPLES

A CML module comprises a DFB laser and an optical band pass filter. The DFB laser is usually biased at around 5 times of its threshold, which provides the benefits of high output power, wide modulation bandwidth and suppression of unwanted transient chirp. The filter is used to adjust the optical signal extinction ratio (ER). Fig.1 (a) shows that the 10-Gb/s PSBT can be generated by directly modulating the CML with a non-return-to-zero (NRZ) electrical signal. The driving voltage V_{pp} is adjusted to induce an adiabatic chirp of $\Delta f = 1/2T$, which generates a phase shift of $\Delta\phi = 2\pi\int_0^T \Delta f(t)dt = 2\pi \times 1/2T \times T = \pi$ during the low level period of the signal, where T is the bit period. The principle of PSBT is the phase shift present in the middle of each "0" bit and the remaining energy resided in consecutive "0"s, as shown in Fig.1 (b). CML based PSBT maintains and even improves the intensity of "1"s and reduces the residual intensity of "0"s through interference, as there exists π phase shift difference between the broadened energy profile of the "1"s and the residual energy within the "0"s at their middle points of the bit periods, no matter the number of "0"s between the "1"s is odd or even, after transmission, as shown in Fig.1 (c). Hence, the chromatic dispersion tolerance as well as the optical reach is greatly enhanced.

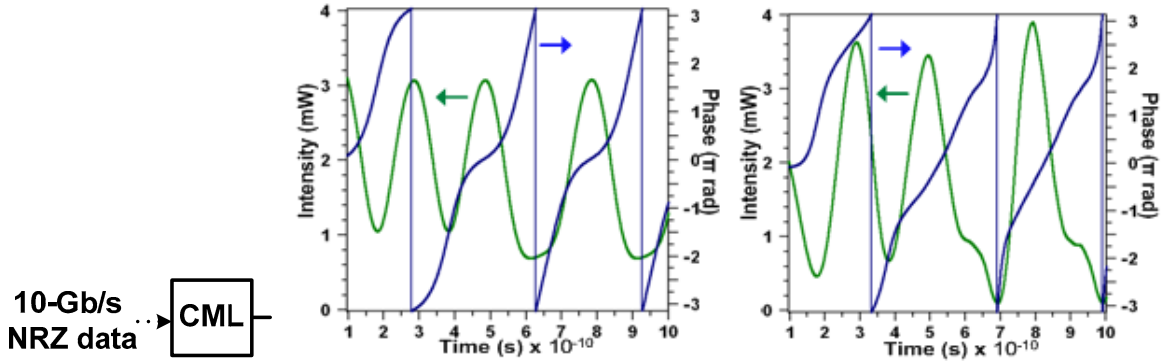

(a) (b) (c)

Fig. 1: (a) 10-Gb/s PSBT transmitter. Intensity and phase profiles of the bit patterns (b) before, and (c) after PSBT transmission

In addition to PSBT transmission, other advanced optical modulation formats can also be generated by means of direct modulation of a CML. Fig. 2 and Fig. 3 illustrate the generation of a 10-Gb/s IRZ-duobinary signal and a10-Gb/s Manchester duobinary signal, respectively. The former one is generated by directly modulating the CML with an IRZ electrical signal, while the latter one is realized by means of driving the CML with an electrical Manchester signal, via an electronic XOR gate [2]. Their respective principles of operation are illustrated in Fig. 2(b) and Fig. 3(b). In either case, the driving voltage V_{pp} is adjusted to induce an adiabatic chirp of $\Delta f = 1/T$.

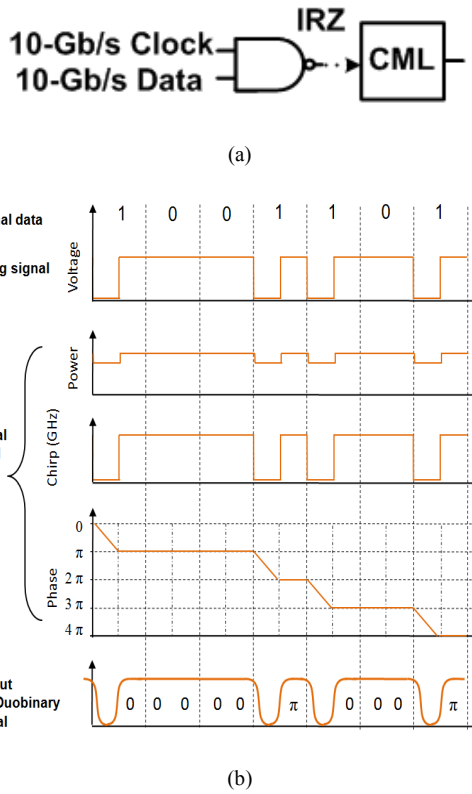

Fig. 2: (a) IRZ-duobinary transmitter. (b) Operation principle.

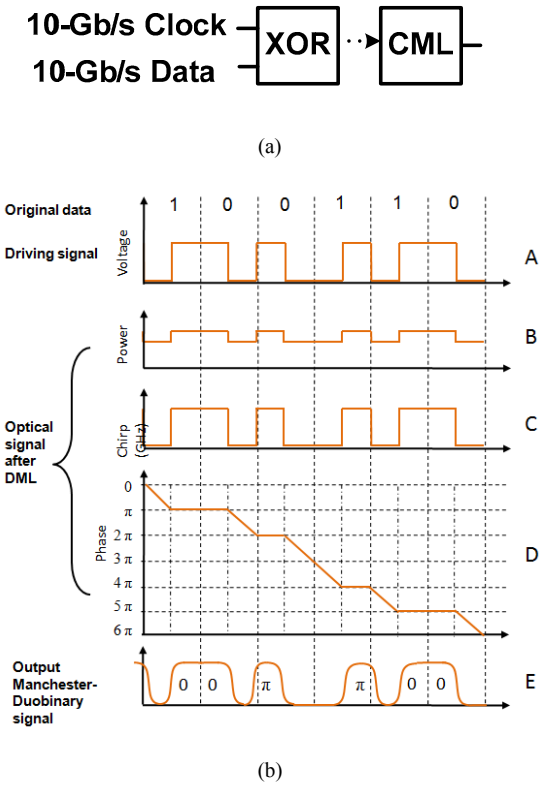

Fig. 3: (a) Manchester-duobinary transmitter. (b) Operation principle.

Similarly, Fig. 4 (a) depicts the generation of a 10-Gb/s RZ-DPSK signal using a CML [3]. The transmitter consists of an IRZ driver, a CML, and a pulse carver. Fig. 4(b) illustrates the operation principle through intensity, frequency and phase characteristics of output signals of the driver, DFB laser (inside CML), filter (inside CML) and pulse carver. The driving voltage V_{pp} is adjusted to induce an adiabatic chirp of $\Delta f = 1/T$. The pulse carver carves the second half-bit of the phase-modulated signal, thus generating the RZ-DPSK signal. The phase modulation is intrinsically differentially encoded. Thus, no differential encoder and phase modulator (PM) are needed. Furthermore, Fig. 5(a) depicts a 20-Gb/s CML-based RZ-DQPSK transmitter consisting of two IRZ encoders, a passive RF combiner, a CML and a pulse carver [4]. Fig. 5(b) illustrates the operation principle through the intensity, chirp and phase characteristics of output signals of the IRZ encoders, RF combiner, DFB laser (inside CML) and pulse carver. The two input data streams are firstly encoded in IRZ format with different driving voltages before being combined by a passive RF combiner to generate a four-level IRZ signal to drive the CML. The pulse carver carves the second half-bit of the phase-modulated signal, thus generating the RZ-DQPSK signal. This scheme could be generalized to generate *M*-ary RZ-DPSK signal based on CML.

(a)

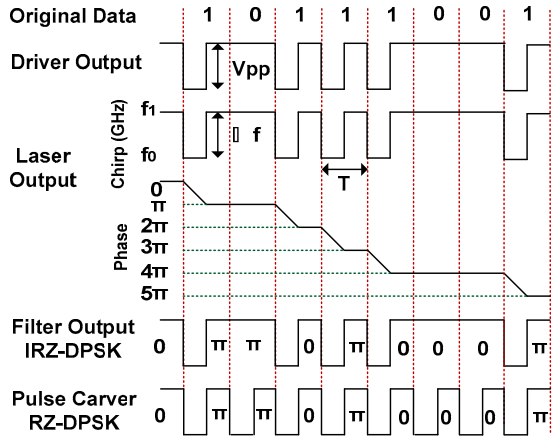

(b)

Fig. 4: RZ-DPSK transmitter, (b) Operation principle.

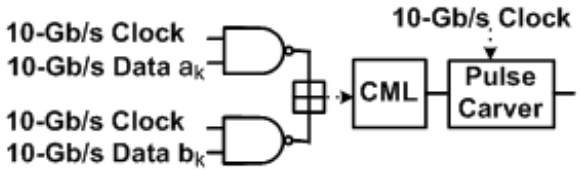

(a)

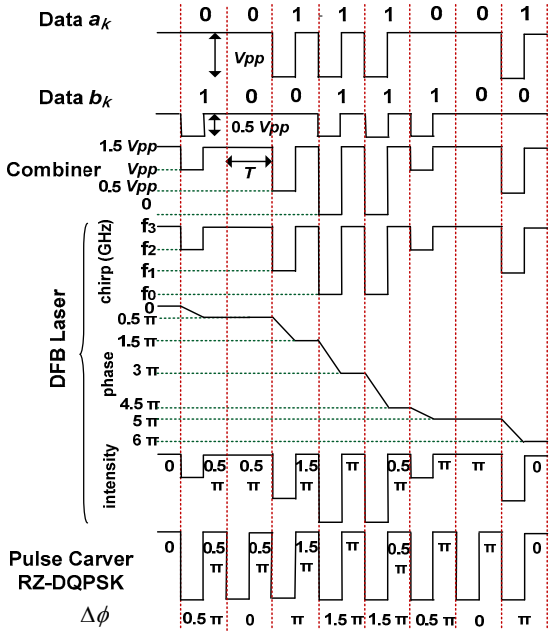

(b)

Fig. 5: RZ-DQPSK transmitter. (b) Operation principle.

3. APPLICATIONS OF CML-BASED FORMATS IN METRO/ACCESS NETWORKS

In this section, applications and transmission performances of different CML-based formats will be discussed.

Application of PSBT

Fig. 6 illustrates the PSBT bit-error-rate (BER) performances and has proved that the transmission can be extended from 50 km to 170 km, 200 km and 220 km, via optimization of signal ER, driving voltage and bias of laser based on a 10-Gb/s 120-km telecom CML. The CML-based PSBT can realize transmission at 10-Gb/s from 0 to 220-km in SSMF without any optical and electrical dispersion compensation, which makes it a promising candidate in optical metro networks.

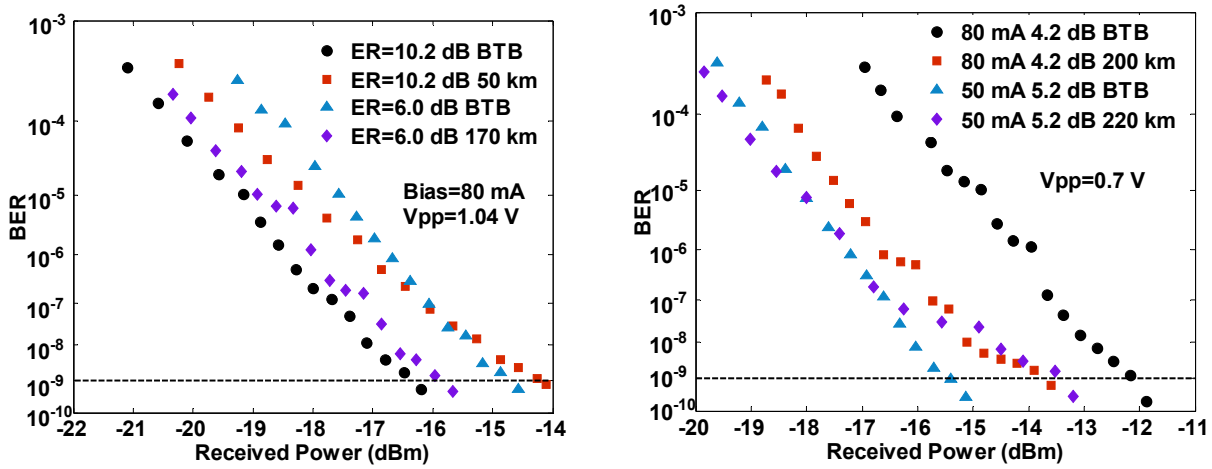

(a) (b)

Fig. 6: BER performance (a) via optimization of ER and (b) via optimization of driving voltage and laser bias. BTB: back-to-back.

Application of IRZ-duobinary format in WDM-PONs

The CML-based IRZ-duobinary format can be employed as the downstream signal format in centralized-light-sources long-reach wavelength division multiplexed passive optical networks (WDM-PONs). The system architecture and the experimental setup are shown in Fig. 7(a) and (b), respectively.

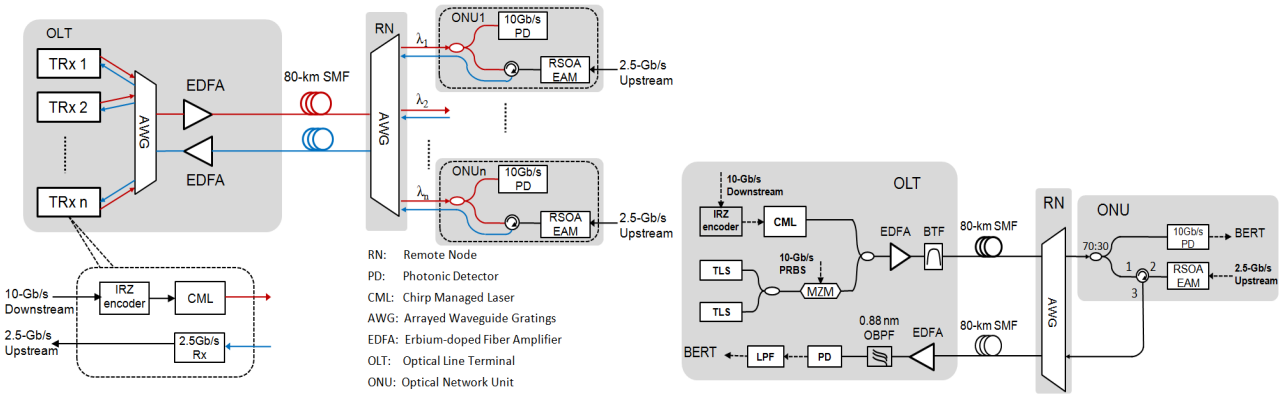

(a) (b)

Fig. 7: (a) Architecture of the WDM-PON with IRZ-duobinary downstream signal. (b) Experimental setup.

As shown in Fig.7 (a), each transceiver at the optical line terminal (OLT) generates its downstream IRZ-duobinary signal and receives its upstream re-modulated signals from its respective subscriber. IRZ coded electrical downstream data is modulated onto a designated wavelength channel through a CML. By properly adjusting the central wavelength of the optical spectrum re-shaper (OSR) integrated in the CML, IRZ-duobinary signal can be obtained. All downstream

modulated wavelengths are multiplexed, via an array waveguide grating (AWG), before being fed into an erbium-doped fiber amplifier (EDFA) for boosting the optical power. Then the downstream wavelengths are delivered to their destined optical network units (ONUs), via a piece of 80-km feeder fiber. At each ONU, an optical coupler splits a portion of the received downstream signal power for detection, while the remaining power is fed into a reflective semiconductor amplifier integrated with electro-absorption modulator (RSOA-EAM) for upstream data re-modulation. The finite optical power in each bit of the received downstream IRZ-duobinary signal provides the light source for 2.5-Gb/s upstream NRZ-OOK data transmission, before being transmitted back to the OLT, via another upstream fiber link. A pair of feeder fibers is used to avoid the possible Rayleigh backscattering induced performance degradation on both the downstream and the upstream signals. At the OLT, the upstream signal is restored by a 2.5-Gb/s optical receiver.

The feasibility of the proposed system has been experimentally assessed on one particular channel for proof-of-concept demonstration. We have also studied the BER performance of the nonlinear crosstalk induced by two co-propagating 10-Gb/s NRZ OOK channels, to simulate multi-channel operation. As illustrated in Fig. 7 (b), a standard CML module (Finisar DM80-01) was used in our experiment. The DML at 1555.63nm was biased at 80 mA and modulated by the electrical IRZ signal with pseudorandom binary sequence (PRBS) with a word length of 2^{31}-1. The V_{pp} of the driving signal was 2.23 volts. The neighboring signals were generated using two tunable laser sources (TLSs) followed by a Mach-Zehnder modulator (MZM), which was also driven by the 10-Gb/s PRBS 2^{31}-1 data. The optical power per channel was adjusted to be equal. The three channels were combined and fed into the EDFA, where each channel was amplified to 6 dBm. The out-of-band noise was suppressed by a bandwidth tunable flat top filter (BTF). At the remote node (RN), an AWG (45 GHz at 3-dB bandwidth) demultiplexed the channels and delivered them to their destined ONUs. At the ONU, an optical coupler was used to split 70% of the received optical power for downstream signal reception, while the rest was amplified and re-modulated by a RSOA-EAM. The upstream signal was then sent back to OLT, via another piece of 80-km fiber, and was restored by a photo-detector (PD), followed by a 5^{th}-order electrical low pass filter (LPF) with 3-dB bandwidth of 1.87 GHz.

Figs. 8 (a) and (b) show the optical eye diagrams of the generated IRZ-duobinary signal, obtained at the output of CML, and that after 80-km transmission, respectively. The duty cycle of the IRZ-duobinary signal was ~60%, which was attributed to the limited modulation bandwidth of the CML. The ER of the signal at the transmitter was 6.7 dB. The relatively low ER was due to the low slope of the OSR in the CML (~11GHz@3dB), and would decrease the receiver sensitivity for the downstream signal. Nevertheless, the downstream signal with low ER provided more optical power for upstream data re-modulation. Fig. 8 (c) and (d) show the optical eye diagrams of the 2.5-Gb/s upstream re-modulated signal at ONU and OLT, respectively. Each upstream symbol contained four downstream symbols. Figs. 8 (e) and (f) show the electrical eye diagrams for the upstream signal after a 1.87-GHz electrical LPF and an inverting amplifier at ONU and OLT, respectively. Clear eye openings were observed.

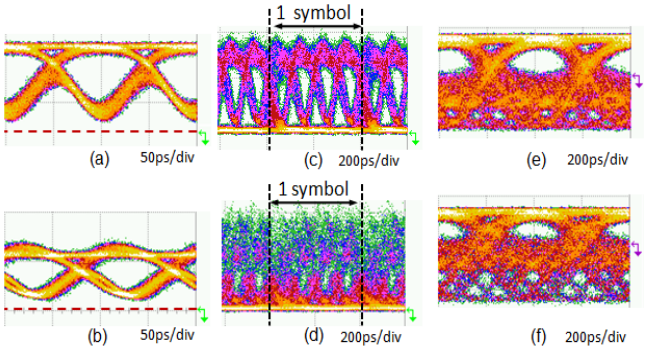

Fig. 8: (a)-(d): Optical eye diagrams of (a) back-to-back IRZ-duobinary signal, (b) IRZ-duobinary signal received at ONU, (c) back-to-back upstream signal at ONU, (d) upstream signal received at OLT. (e)-(f): Electrical eye diagrams of (e) back-to-back upstream signal at ONU, and (f) upstream signal received at OLT.

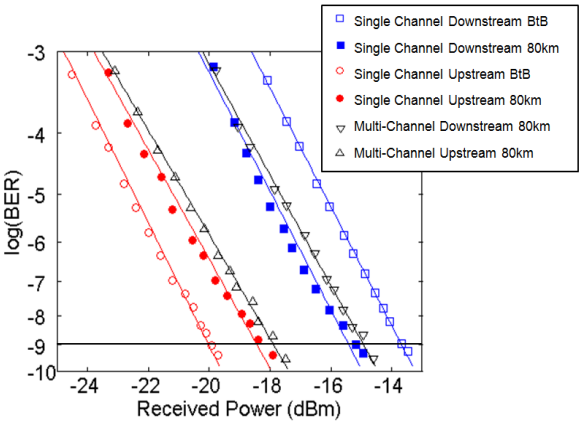

Fig. 9: BER measurements of the 10-Gb/s downstream and the 2.5-Gb/s upstream signals

Fig. 9 shows the measured BER curves. Error-free transmissions were achieved for both the downstream and the upstream signals, after 80.4-km standard single-mode fiber (SSMF) transmission without dispersion compensation. The back-to-back (BtB) sensitivity (at BER of 10^{-9}) for the 10-Gb/s downstream IRZ-duobinary signal and the 2.5-Gb/s upstream re-modulated NRZ-OOK signal were measured to be -13.67 dBm and -20.07 dBm, respectively. After 80.4-km transmission, their respective sensitivities were measured to be -14.96 dBm and -17.88 dBm, giving -1.29-dB and 2.19-dB penalty. The performance of single-channel operation was also measured in order to determine the penalty induced by multi-channel transmission. The single channel sensitivity (at BER of 10^{-9}) for the downstream signal received at ONU and the upstream signal at OLT were -15.12 dBm and -18.21 dBm. Small penalties were observed. Error-free transmissions for both the downstream and the upstream signals have been achieved without dispersion compensation.

Improved dispersion tolerance of Manchester-duobinary signal

The 10-Gb/s CML-based Manchester-duobinary signal increases the chromatic dispersion (CD) tolerance of the Manchester signal by three times, which makes it applicable in burst mode transmission and bi-directional access networks [3]. The experimental setup of CD tolerance measurement is shown in Fig. 10. A standard CML module (Finisar DM80-01) was employed in our experimental setup. The DFB-LD at 1554.60 nm was biased at 75 mA and was modulated by an 10-Gb/s electrical Manchester signal with PRBS and a word length of 2^{31}-1. The V_{pp} of the driving signal was 2.25 V. Different lengths of dispersion-compensation module or SSMF with ~17 ps/(nm·km) chromatic dispersion were utilized to study the chromatic dispersion tolerance of the optical Manchester-duobinary signals. The optical power of the Manchester-duobinary signal was kept below 0 dBm, in order to avoid the impact from fiber nonlinearity. Single PD was used for signal detection.

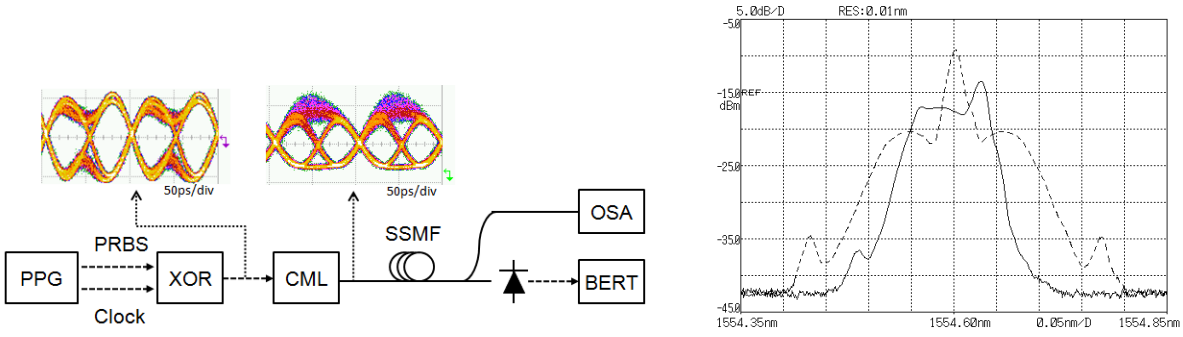

(a) (b)

Fig. 10: (a) Experimental setup. (b) Optical spectra of 10-Gb/s conventional Manchester (dashed line) and Manchester-duobinary (solid line) signals.

Fig. 10 (b) shows the optical spectrum of the generated 10-Gb/s CML-based Manchester-duobinary signal (solid line) and it was compared with that of the 10-Gb/s conventional Manchester signal (dashed line). The tone of CML-based Manchester duobinary signal was shifted and the carrier was suppressed. The 20-dB bandwidths of the Manchester-duobinary signal and conventional Manchester signal were measured to be 18 GHz and 29 GHz, respectively. The Manchester-duobinary signal exhibited relatively more compact spectrum, as compared with that of a conventional Manchester signal. Thus it gave better tolerance against fiber chromatic dispersion in optical fiber transmission. The insets in Fig.10 (a) shows the eye diagrams of the electrical driving signal and the output optical signal. The ER of the output optical signal was 8.7 dB. The relative low ER was attributed to the low slope of the OSR in the CML (~11GHz@3dB).

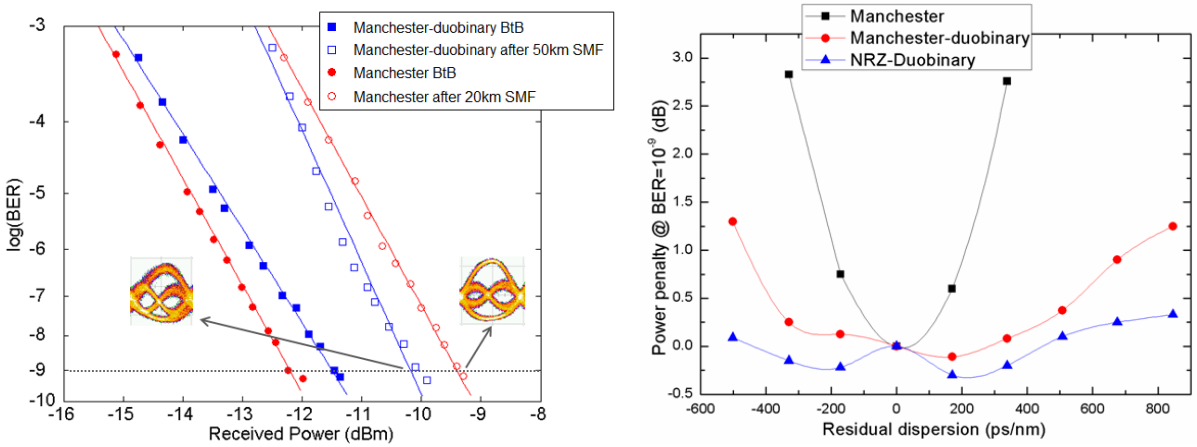

(a) (b)

Fig. 11: Experimental measurements for 10-Gb/s Manchester-duobinary signal and conventional Manchester signal. (a) BER performance, (b) chromatic dispersion tolerance.

As shown in Fig. 11(a), the back-to-back sensitivities (at the BER of 10^{-9}) for 10-Gb/s Manchester-duobinary signal and conventional Manchester signal were -11.45 dBm and -12.23 dBm, respectively. The 0.78-dB difference was mainly attributed to relatively low ER and overshoot of the Manchester-duobinary signal. The relatively low receiver sensitivities were mainly due to the insufficient electrical preamplifier gain in the photodetector. The power penalty of the Manchester-duobinary signal after 50-km SSMF transmission was 1.31 dB while that of the conventional Manchester signal after only 20-km SSMF transmission was 2.80 dB, showing the much longer optical reach for the Manchester-duobinary signal. We have also investigated and compared the chromatic dispersion tolerance between the Manchester-duobinary format and the conventional Manchester format. Fig. 11(b) depicts their respective power penalties (at BER=10^{-9}) measured at different residual chromatic dispersions. It was found that the 10-Gb/s Manchester-duobinary signal exhibited dispersion tolerance from -460 ps/nm to +720 ps/nm, at 1-dB power penalty. However, under the same condition, the 10-Gb/s conventional Manchester signal only exhibited dispersion tolerance from -190 ps/nm to +200 ps/nm, at 1-dB power penalty. The measurements showed that dispersion tolerance of the Manchester-duobinary format was around three times superior to that of the conventional Manchester signal.

***Experimental results of RZ-DPSK and RZ-DQPSK* signals**

Fig. 12 shows the BtB eye diagrams of the IRZ driving signal after the driver, IRZ-DPSK signal after CML, RZ-DPSK signal after the pulse carver and demodulated RZ-DPSK signals at the two ports of the delay interferometer (DI). The double line of RZ-DPSK signal, shown in Fig.12(c), was due to the limited rising and falling time of the driving signal, as in Fig. 12(a), and non-ideal modulation response of DFB laser in CML[4], denoted in Fig. 12(b). Demodulated RZ-DPSK signal at the destructive port of the DI, shown in Fig. 12(d), had better performance than the one at the constructive port of DI, as in Fig. 12(e), mainly attributed to the asymmetric shape, the noise of the driving signal and the non-ideal modulation response of the DFB laser in the CML.

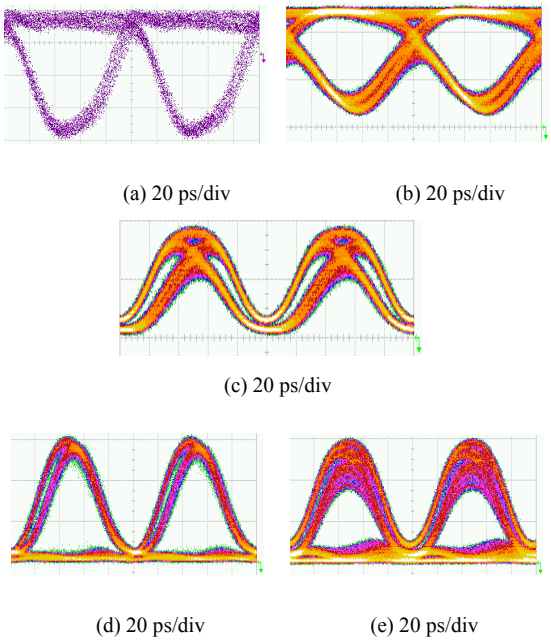

Fig. 12: Eye diagrams of (a) IRZ driving signal, (b) IRZ-DPSK signal, (c) RZ-DPSK signal, (d) demodulated RZ-DPSK signal at the destructive port of DI, (e) demodulated RZ-DPSK signal at the constructive port of DI.

Fig. 13(a) depicts the receiver sensitivities at BER=10^{-9} measured after various lengths of SSMF transmission. The insets of Fig. 13(a) show that CML based RZ-

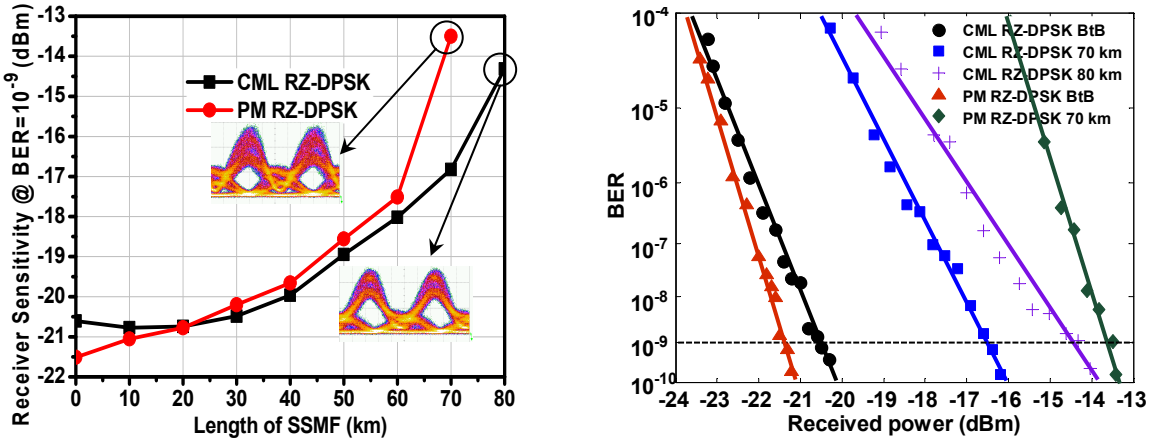

(a) (b)

Fig. 13: Measured chromatic dispersion tolerance for CML and PM based RZ-DPSK signals. Insets shows the respective eye diagrams after 70-km SSMF transmission. Time scale: 20 ps/div. and (b) BER measurements for CML and PM based RZ-DPSK signals.

DPSK signal had much clearer eye diagram than PM based RZ-DPSK signal after 70-km SSMF transmission. Fig.13 (b) shows the measured BER performances. The BtB receiver sensitivities for CML and PM based RZ-DPSK signals were -20.6 dBm and -21.5 dBm, respectively. 80-km error free SSMF transmission was achieved for CML based 10-Gb/s RZ-DPSK signal, while the PM based 10-Gb/s RZ-DPSK signal could only be transmitted up to 70 km with error-free performance. The CML-based RZ-DPSK signal can benefit from high receiver sensitivity using balanced detection and high nonlinearity tolerance, suitable for long-reach access network which requires high performance.

CML-based 20-Gb/s RZ-DQPSK could meet the increasing capacity demand in metro networks with the features of high receiver sensitivity, high nonlinearity robustness and high bandwidth efficiency [5]. Fig. 14 shows the experimental (upper) and simulated (lower) back-to-back (BtB) eye diagrams of the signals after the RF combiner, CML, pulse carver and demodulated data a_k signal at one port of the DI. Fig. 15 shows the waveform traces measured by a real-time oscilloscope. Two data sequences a_k=00111001 and b_k=10011100 were applied to the transmitter. The subtraction of the bottom and top demodulated waveforms, shown in Fig. 15(c), would correctly regenerate the input bit sequence a_k. Decoding of $b_k=p_k \oplus q_k$ would also regenerate the input bit sequence b_k, as shown in Fig. 15(c) and (d).

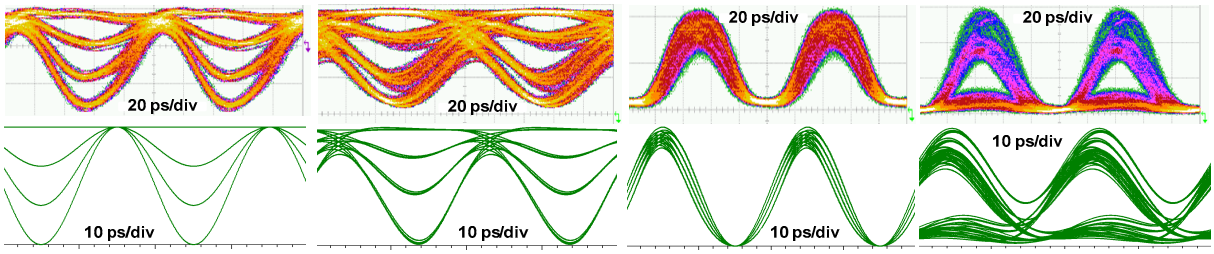

(a) (b) (c) (d)

Fig. 14: Experimental (upper) and corresponding simulated (lower) eye diagrams of (a) signal after the RF combiner, (b) signal after the CML, (c) RZ-DQPSK signal after the pulse carver and (d) demodulated data a_k signal at one port of the DI.

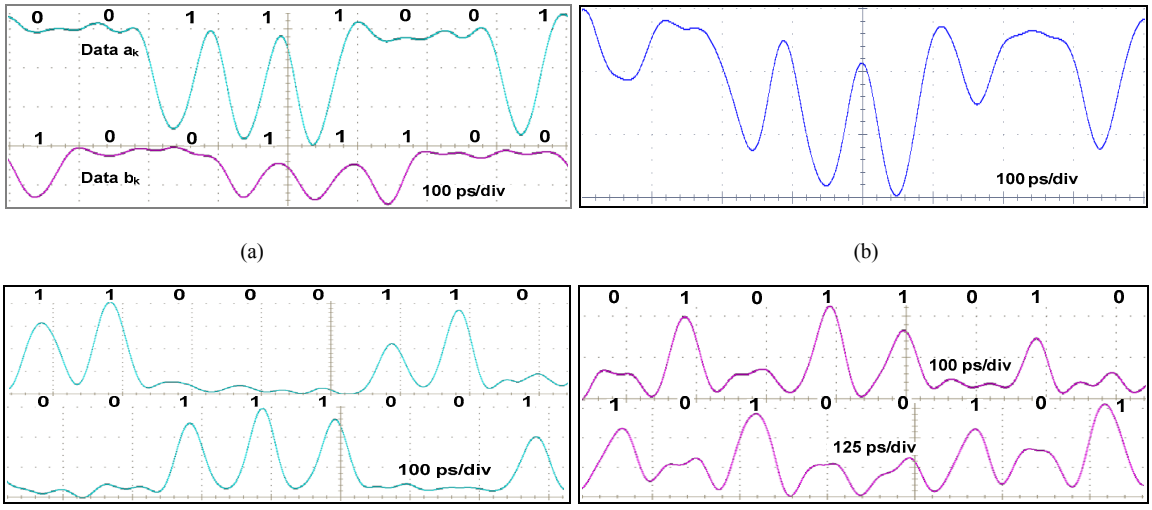

(a) (b)

(c) (d)

Fig. 15: Waveform traces for signals (a) of data a_k and b_k, (b) after the RF combiner, (c) of demodulated data p_k and (d) of demodulated data q_k.

4. SUMMARY

We have discussed the generation of various advanced modulation formats using a directly modulated CML at 10-Gb/s and above. The CML-based transmitters have the benefits of more compactness, lower cost, higher performance and less power consumption compared with the conventional ones. These CML-based modulation formats have exhibited larger chromatic dispersion tolerance, and their transmitters are more cost-effective. Their attractive features make them suitable for various kinds of applications in optical metro/access networks.

REFERENCES

[1] Y. Matsui, D. Mahgerefteh, X. Zheng, C. Liao, Z.F. Fan, K. McCallion, and P. Tayebati, "Chirp-managed directly modulated laser (CML)," *IEEE Photonics Technology Letters*, 18(2), 385-387 (2006).

[2] D. Mahgerefteh, Y. Matsui, X. Zheng, and K. McCallion, "Chirp managed laser and applications," *IEEE Journal of Selected Topics in Quantum Electronics*, 16(5), 1126-1139 (2010).

[3] Z. Liu, and C.K. Chan, "Generation of dispersion tolerant Manchester-duobinary signal using directly-modulated chirp managed laser," *IEEE Photonics Technology Letters*, 23(15), 1043-1045 (2011).

[4] W. Jia, J. Xu, Z.X. Liu, K.H. Tse, and C.K. Chan, "Generation and transmission of 10-Gb/s RZ-DPSK signals using a directly modulated chirp managed laser," *IEEE Photonics Technology Letters*, 23(3), 173-175 (2011).

[5] W. Jia, J. Xu, Z.X. Liu, C.K. Chan, and L.K. Chen, "Generation of 20-Gb/s RZ-DQPSK signal using a directly modulated chirp managed laser," OFC/NFOEC 2011, Paper OThE4, LA CA, USA (2011).